BULLETIN OF THE POLISH ACADEMY OF SCIENCES
TECHNICAL SCIENCES, Vol. 74(1), 2026, Article number: e156796
DOI: 10.24425/bpasts.2025.156796

Aerodynamic performance optimization of a vertical-axis wind turbine using blade-spoke connection and pitch angle via the Taguchi method

Himmet Erdi TANÜRÜN*

Kahramanmaraş İstiklal University, Elbistan Engineering Faculty, Department of Energy Systems Engineering, Elbistan, Kahramanmaraş, Türkiye

Abstract. In this study, the effect of various parameters on the power coefficient (C_P) performance of a vertical axis wind turbine (VAWT) was optimized using the Taguchi method. The optimization was conducted with the Taguchi method, employing three control factors: blade-spoke connection (BSC), turbine blade pitch angle (β), and turbine blade pitch direction (φ). Subsequently, the analysis of variance (ANOVA) method was employed to determine the contribution ratio of each control factor. Regression analysis (RA) was applied to develop an empirical equation predicting the C_P of the VAWT, incorporating the control factors. The results indicated an optimal parameter configuration of BSC = 0.5c, $\beta = 2°$, and φ = (-), which maximizes the system performance. The performance of the optimal model was observed to exceed that of the conventional VAWT (B1) by 5.82%. Using the ANOVA method, the contribution of parameters on the C_P performance of the VAWT was ranked as follows: φ > BSC > β. The φ parameter has the most significant effect at 82.07%, whereas the β parameter exhibits the least effect of 1.17%. Moreover, the predictive accuracy of the developed regression model was validated, yielding R^2 values of 0.9221 for the training data and 0.9908 for the test data.

Keywords: analysis of variance (ANOVA); computational fluid dynamics (CFD); confirmation test; power coefficient (C_P); wind energy.

1. INTRODUCTION

The increasing global energy demand underscores the urgent need to adopt sustainable and environmentally friendly alternatives in energy production [1]. Fossil fuels, which have long dominated the energy sector, are associated with various adverse effects, including greenhouse gas emissions, air pollution, resource depletion, and environmental degradation [2,3]. These environmental and economic concerns have accelerated the shift toward renewable energy technologies [4]. In this context, wind energy systems emerge as a prominent solution due to their massive electricity generation and long-term availability [5,6]. Wind turbines are classified into two main types, horizontal axis wind turbines (HAWTs) and vertical axis wind turbines (VAWTs), in accordance with the orientation of their rotational axis [7,8]. HAWTs have traditionally dominated the wind energy market owing to their high aerodynamic efficiency and mature technological development [9,10]. However, in complex terrains and urban environments characterized by highly turbulent and multidirectional wind flows, the performance of HAWTs can be significantly limited [11]. VAWTs, on the other hand, offer key advantages such as omnidirectionality [12], producing energy at low rotational speeds, and featuring compact configurations [13]. The absence of yaw mechanisms simplifies the mechanical design and potentially reduces maintenance requirements. Owing to their low noise levels, compact structure, ease of maintenance [14], and low center of gravity [15], small-scale VAWTs can be effectively integrated into buildings, particularly for rooftop applications, where their structural stability and ability to operate under turbulent wind conditions [16] make them ideal for urban micro-generation [17]. In recent years, the considerable growth of both academic and industrial interest in VAWT systems has led to extensive research focusing on the aerodynamic performance of Darrieus wind turbines. In these studies, numerical and experimental approaches, with optimization studies conducted to maximize power output, have thoroughly investigated the effects of various geometric and operational parameters, such as the number of blades [18], blade pitch angle (β) [19], Reynolds number [20], turbulence characteristics [21], blade profile effect [22,23], and solidity [24,25].

In the realm of VAWTs, various design elements significantly contribute to overall performance. The blade-spoke connection (BSC) is a critical element in the VAWT design, with a noteworthy influence on power efficiency by altering aerodynamic properties and mechanical stability of the rotor. A strategically optimized connection position could significantly enhance VAWT performance, extending operational longevity and augmenting energy output. Alongside the BSC, another important parameter is the β of the turbine blades. The β determines how the blade interacts with the incoming wind and directly influences the turbine power coefficient (C_P), which reflects its efficiency in converting wind energy into mechanical power.

To conduct a comprehensive and systematic literature review on the aerodynamic and structural effects of two key design parameters, namely the β and the BSC, on VAWTs, this study employed the Preferred Reporting Items for Systematic Reviews

*e-mail: erdi.tanurun@istiklal.edu.tr

Manuscript submitted 2025-07-09, revised 2025-10-19, initially accepted for publication 2025-10-23, published in January 2026.

and Meta-Analyses (PRISMA) framework. The PRISMA process includes five main steps: setting inclusion criteria, identifying relevant sources, conducting a literature search, extracting necessary data, and selecting eligible studies. Originally proposed by Moher *et al.* [26], PRISMA has found widespread application in various fields such as health sciences [27] and environmental sciences [28], and has recently gained traction in wind energy research as well [7]. By applying this systematic methodology, the literature review in this study was conducted more comprehensively and objectively than traditional approaches, thereby utilizing quantitative evidence to reinforce the originality of the study. As seen in Table 1, in the first stage of the systematic literature review, a comprehensive search was performed in the Scopus database using the combined keywords "vertical AND axis AND wind AND turbine," and "blade AND spoke AND connection," or "blade-spoke AND connection," or "strut." using the TITLE-ABS-KEY format (referred to as TAK). This query yielded a total of 67 studies, as shown in Query 1. While most studies retrieved using the keyword "strut" focused on load force distribution and structural strength analysis, only a few addressed aerodynamic performances. Specifically, only a limited number of these studies addressed the aerodynamic effects of strut and blade-spoke configurations in relation to turbine efficiency.

To further refine the scope in line with the present study, the keyword "NACA 0021", corresponding to the airfoil used in this research, was added to the search. As illustrated in Query 2, this reduced the number of relevant publications to only 2. Additionally, in Query 3, optimization-focused terms such as "ANOVA" and "Taguchi" were included, and no relevant studies were observed. In Query 4, the keywords "pitch angle" and "vertical AND axis AND wind AND turbine" were added, resulting in 135 studies. Subsequently, in Query 5, the addition of "Taguchi" and "ANOVA" further refined the results to only 5 relevant studies. In Query 6 and Query 7, "NACA 0021" and "blade-spoke connection" were individually added to the keywords of Query 5, but no studies were found. Consequently, the PRISMA-based systematic review was concluded by focusing on studies related to BSC, β, and Taguchi-based β optimization. After additional filtering based on language (English only), access (open-access only), and application area (excluding marine-related studies), a total of eight studies were identified as directly relevant to the BSC, strut, and β configuration in VAWTs.

The BSC is a vital component influencing both the aerodynamic efficiency and mechanical integrity of VAWTs. Optimizing its position can enhance performance and reduce losses. Franchina *et al.* [29] and Keisar *et al.* [30] emphasized the impact of blade-strut interactions and offset (x_c/c) on torque and dynamic stall. Hara *et al.* [31] and Jiang *et al.* [32] showed that airfoil-shaped struts and tip-positioned supports improve performance, achieving a 9.05% increase in power output. Aihara *et al.* [33] noted up to 43% CP loss due to struts, although the effect of the central tower was found to be minimal. Santamaría *et al.* [34] and Aihara *et al.* [35] confirmed parasitic drag effects using ADM and RANS/vortex models, which resulted in approximately 24% efficiency reduction. Miao *et al.* [36] reported that elliptical struts with optimized geometry reduced drag by 25.8%. Similarly, β has a direct effect on C_P by modifying blade-wind interactions. Ribeiro [37] and Santamaría *et al.* [38] showed that β influences wake steering, but its effect on pitching moments was found to be negligible. Bianchini *et al.* [39] and Yang *et al.* [19] observed pressure and torque improvements at specific β values. Xu *et al.* [40] reported a 78.6% C_P gain with optimized β, while Elsakka *et al.* [41] and Ardaneh *et al.* [42] found that sinusoidal and negative fixed β reduced drag and stall. Hunt *et al.* [43] and Ma *et al.* [44] highlighted

Table 1
Systematic literature review using selected keywords in SCOPUS

Query	Search details	Number of studies
1	TAK (vertical AND axis AND wind AND turbine) AND TAK (blade AND spoke AND connection) OR TAK (blade-spoke AND connection) OR TAK (strut)	67
2	TAK (vertical AND axis AND wind AND turbine) AND TAK (blade AND spoke AND connection) OR TAK (blade-spoke AND connection) OR TAK (strut) AND TAK (NACA 0021)	2
3	TAK (vertical AND axis AND wind AND turbine) AND TAK (blade AND spoke AND connection) OR TAK (blade-spoke AND connection) OR TAK (strut) AND TAK (NACA 0021) AND TAK (taguchi) OR TAK (ANOVA)	N/A
4	TAK (vertical AND axis AND wind AND turbine) AND TAK (pitch AND angle)	135
5	TAK (vertical AND axis AND wind AND turbine) AND TAK (pitch AND angle) AND TAK (taguchi) OR TAK (ANOVA)	5
6	TAK (vertical AND axis AND wind AND turbine) AND TAK (pitch AND angle) AND TAK (taguchi) OR TAK (ANOVA) AND TAK (NACA 0021)	N/A
7	TAK (vertical AND axis AND wind AND turbine) AND TAK (pitch AND angle) AND TAK (taguchi) OR TAK (ANOVA) AND TAK (NACA 0021)	N/A
8	TAK (vertical AND axis AND wind AND turbine) AND TAK (pitch AND angle) AND TAK (blade AND spoke AND connection) OR TAK (blade-spoke AND connection) AND TITLE- AND TAK (taguchi) OR TAK (ANOVA)	N/A

toe-out and constant-AoA β strategies, achieving notable C_P increases.

To evaluate the interplay between multiple parameters, the Taguchi method has been effectively employed in several studies. Taguchi-based studies further confirmed the importance of β. Peng *et al.* [45,46] found ~ 13% C_P gains at optimal β in twin-VAWT configurations. Zhang *et al.* [47] doubled output in hybrid systems via β tuning. Rasekh *et al.* [48] identified β amplitude and shift as key factors, and Lu and Xu [49] optimized $\beta = -2.47°$ via a hybrid Taguchi-Kriging-JADE approach, achieving 4.5% improvement.

As seen in the aforementioned studies, there have been many recent investigations into the effect of both the BSC and the β on the C_P performance of VAWTs. While β is frequently studied as a parameter for aerodynamic control and efficiency enhancement, the BSC is addressed from a structural integrity or drag-reduction perspective rather than within a performance optimization context. Studies such as Franchina *et al.* [29], Hara *et al.* [31], and Miao *et al.* [36] focused on the aerodynamic effects of different strut geometries and connection strategies, revealing their influence on flow structures, especially near the blade-strut junction, and highlighting that inappropriate BSC configurations can lead to significant performance losses. For instance, Miao *et al.* [36] demonstrated that strut shape and placement can alter the flow topology and reduce drag by up to 25.8% using a novel elliptical profile.

On the other hand, several studies, such as Yang *et al.* [19], Ardaneh *et al.* [42], and Ma *et al.* [44], explored the role of β in enhancing C_P by adjusting fixed or active β strategies. These studies demonstrated that tuning the β can delay stall, smooth out torque output, and optimize aerodynamic loading, especially at lower tip speed ratios (TSRs or λ). Notably, Ma *et al.* [44] reported an average 13.46% increase in C_P by implementing a constant AoA strategy using active β control. Although the Taguchi method, a widely accepted statistical optimization approach, is implemented in studies such as Peng *et al.* [45] and Zhang *et al.* [47], these works primarily focused on β, solidity, airfoil selection, and rotational configuration. The BSC is not incorporated as a design parameter in any of these optimization frameworks. Furthermore, among all these efforts, only Zhang *et al.* [47] integrate variance analysis (ANOVA) into the optimization pipeline to quantify the relative influence of each parameter. This indicates that a comprehensive approach integrating both BSC and β within an optimization algorithm, supported by ANOVA and confirmation tests, has not yet been presented in the literature. Therefore, the absence of a study that simultaneously evaluates both BSC and β, especially under a systematic and statistical optimization framework, represents a significant gap in the VAWT literature, particularly in terms of aerodynamic performance improvement.

In this study, the aerodynamic performance of a VAWT was evaluated by examining the combined effects of BSC, β, and φ, a combination that has not been previously investigated within a unified optimization framework. The Taguchi method was employed to systematically determine the most influential parameter levels for maximizing the C_P. Unlike earlier works that treated BSC and β independently, this study is the first to include both as simultaneous design variables in a statistical design of experiments (DOE) setting. The significance of each factor was assessed using ANOVA, while a regression model was developed to predict C_P as a function of the selected parameters. The reliability of the model and optimization strategy was confirmed through verification tests. Finally, this work not only introduces a novel combination of design variables in VAWT optimization but also offers a replicable framework for future design improvements aimed at enhancing turbine efficiency.

After presenting the background, motivation, and importance of the study, the remaining parts are organized as follows: Section 2 introduces the materials and methods employed in this research, including the physical model, numerical method, independence analysis of turbine revolution and time step, and verification process. Section 3 explains the Taguchi method used for the optimization procedure. Section 4 presents the results and discussion, detailing the factor and S/N effects of VAWT, ANOVA, correlation, and confirmation tests, and aerodynamic examination. Finally, Section 5 provides the conclusions, summarizing the key findings and highlighting the main contributions of the study.

2. MATERIAL AND METHOD

2.1. Physical model

The study aimed to utilize the National Advisory Committee for Aeronautics (NACA) 0021 blade model to optimize the C_P performance of the VAWT. The NACA 0021 airfoil demonstrated favorable lift characteristics and stable torque output across a wide range of TSRs, resulting in improved aerodynamic performance in both numerical and experimental studies. Due to these advantages, it is widely adopted in the literature as a reference model for VAWTs [50–52]. D and c used in the turbine model were set at 1030 mm and 85.8 mm, respectively. An inner zone was designed to simulate the movement of the vertical axis blades during the turbine rotation. Within this inner zone, three distinct areas were created to enhance analysis of each blade: control circle 1 (cc1), control circle 2 (cc2), and control circle 3 (cc3). Each of these zones was established to encapsulate each blade separately. To prevent the computational domain from impacting the performance of the flow, appropriate dimensions were defined. According to existing research [53], the distances from the turbine center to the inlet, outlet, and lateral-top boundary conditions were set at 6D, 12D, and 5D, respectively, as shown in Fig. 1.

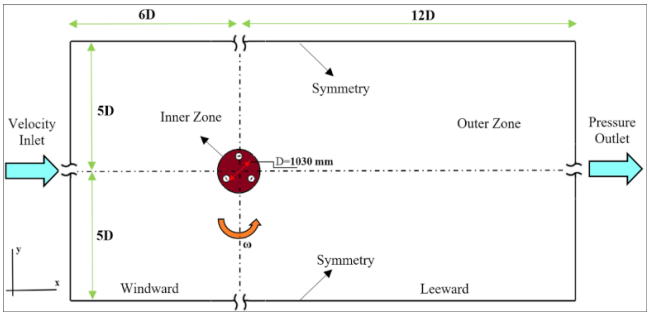

Fig. 1. Schematic representation of the computational domain

The free stream velocity (U_0) of air at the inlet was set to 9 m/s for this study. The outlet condition was determined to be atmospheric, while symmetry and no-slip conditions were assigned to the lateral and top boundaries. Interfaces were constructed between each zone to ensure continuity of flow across the zones. The study was conducted with a turbulence intensity (TI) of 1% and a fluid density (ρ) of 1.225 kg/m^3. The conventional VAWT parameters were taken from the configuration validated by Castelli *et al.* [50], and were used as the B1 in this study.

2.2. Numerical method

The SST (shear stress transport) turbulence model is a widely used turbulence model in the field of computational fluid dynamics (CFD), including applications related to wind turbines [54]. The SST model provides improved accuracy compared to simpler turbulence models, making it a valuable tool in wind turbine design and optimization [53, 55, 56].

The efficiency of VAWTs is strongly influenced by their torque and power generation characteristics, which depend on the aerodynamics of the blades interacting with the incoming wind. As can be seen in (1) and (2), these parameters can be directly related to the size, shape, and rotational speed of the turbine.

$$T = \int r \, \mathrm{d}F, \tag{1}$$

$$P = \omega T, \tag{2}$$

where $\mathrm{d}F$ is the force vector from the axis of rotation to the point of force application, ω is the angular velocity, and r is the position vector.

The C_P shown in (3) is a measure of the efficiency of a wind turbine [57, 58]. It is the ratio of the power extracted by the turbine to the total power available in the wind resource at a given wind speed. C_P can be calculated using the following formula

$$C_P = \frac{P}{\left(0.5\rho A U_\infty^3\right)}, \tag{3}$$

where A is the swept area of the turbine blades, and U_∞ is the wind speed at the turbine.

The TSR or λ, defined in (4), is a crucial parameter in the operation of VAWTs. It is the ratio of the tangential speed of the blade tip to the free-stream wind speed. Optimal energy capture is achieved when the TSR is within a specific range, which depends on the specific design of the VAWT [56, 59]

$$\mathrm{TSR}(\lambda) = \frac{(\omega R)}{(U_\infty)}. \tag{4}$$

In this study, Fig. 2 presents the mesh grid distribution of the VAWT used for validation. Within the flow domain, mesh sizes progressively increase from the vicinity of the turbine blades towards the inlets, outlets, and outer wall. This design meets the requirement for a more detailed solution near the turbine. Triangular grids were applied in the control areas cc1, cc2, and cc3 using Ansys meshing, whereas quadrilateral grid methods were used in the other regions of the computation area. The variability of flow characteristics near the surface of the turbine blades necessitates the use of a triangular structure to ensure the attainment of an accurate solution, even though it extends the solution time. Figure 2 illustrates the mesh structure used in the simulation, highlighting the mesh characteristics in different regions of the computational domain, including the hub, enclosure, around the blade, and the cc1 control surface. To accurately solve this flow phenomenon, grid boundary layers were established on the blade surface. The first boundary layer, known as y^+, is used to monitor the transitionquality of the boundary layer and is intended to be less than 1 in external flow applications, as noted in previous studies [60, 61]. In this study, the growth rate of 1.2. was used to achieve a y^+ value of less than 1, twelve boundary layers were created.

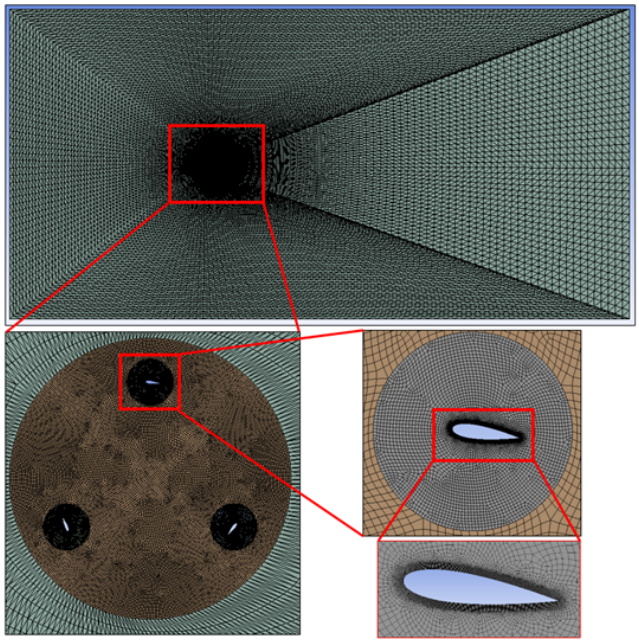

Fig. 2. (a) Computational domain (b) hub region (c) control circle region d) computational near turbine blade

2.3. Independence from the turbine number of revolutions and time step

Accuracy in CFD studies necessitates testing factors like time step, revolution number, and mesh size. Employing a smaller time step, often represented as the blade azimuth increment ($\Delta\Omega$), results in an exponential rise in computational cost. Thus, the identification of an optimal time step is crucial [54]. The impact of C_P on a straight VAWT at a TSR of 2.62 was evaluated for six distinct azimuth increments, ranging from 0.5 to 8°, as depicted in Table 2. The findings illustrate noticeable discrepancies in the C_P attained at larger $\Delta\Omega$ values, such as 2°, 4°, and 8°. Nonetheless, the obtained C_P error rate between 1° and 0.5° is approximately 1%, with all analyses in this study fixed at 1°, aligning with the existing literature.

Revolution independence in VAWTs is paramount in maintaining consistency and stability during the turbine operation, a

Table 2
Sensitivity of C_P to azimuthal step size for straight-VAWT at TSR = 2.62 [11]

$\Delta\varphi$	C_P	Error rate (%)
8°	0.357368	
4°	0.335444	6.535
2°	0.327875	2.308
1°	0.324132	1.154
0.5°	0.322010	0.659

notion backed by various scientific studies. In this study, the numerical analysis of 16 different models created using the Taguchi orthogonal design was performed. While the values of rotational independence attained by each model are similar, they are not identical. However, to guarantee rotational independence, all models performed 15 rotations at a 1° azimuth angle, a method widely accepted in the literature. The C_M graph for B1 over 15 revolutions is displayed in Fig. 3. The error rate between the last four rotations for all models is less than 1%, which is very consistent with the literature.

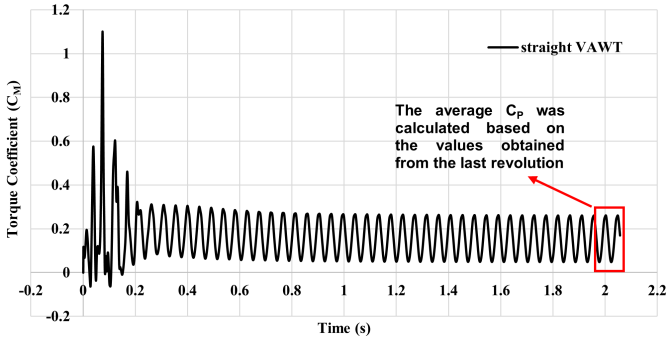

Fig. 3. C_M vs revolution time graph of conventional VAWT (B1)

Figure 4 presents the alteration in C_P of the B1 across eight different mesh counts, ranging from 50 to 310×10^3. Observations based on Fig. 4 indicate that no significant fluctuations were noticed in the C_P beyond the mesh count of 190×10^3. Thus, a mesh count of approximately 190×10^3 was employed in all subsequent numerical analyses.

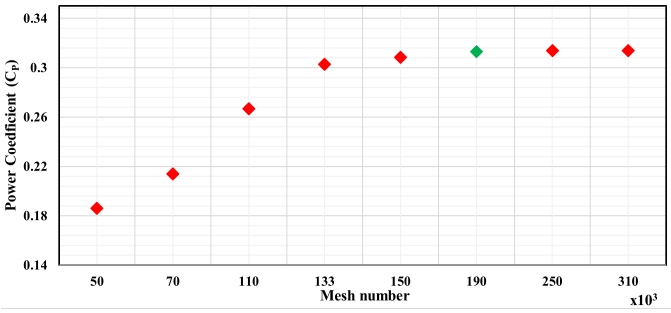

Fig. 4. C_P mesh independence study for the straight VAWT at TSR of 2.62 [11]

2.4. Verification

The verification process in two-dimensional (2D) numerical analysis is of importance for the accuracy and reliability of the numerical work conducted. In this context, the present 2D simulation was verified by comparing its outcomes with both experimental and numerical results available in the literature. In this study, the verification process was conducted using experimental and 2D numerical studies by Castelli *et al.* [50], as well as the 2D numerical studies by Ni *et al.* [62] and Hassanpour and Azadani [63], as shown in Fig. 5. Upon examining the results, it was observed that the C_P values at all TSRs obtained in this study were consistent with Castelli *et al.* [50] experimental and Ni *et al.* [62] numerical work. Particularly, at a 2.62 TSR, where the optimal value was achieved and which was used in all models in this study, a flawless similarity was obtained with the results of both Castelli *et al.* [50] and Ni *et al.* [62]. At TSR = 2.62, the percentage error was found to be approximately 4.9%, while higher discrepancies of 6.0% and 15.0% were observed at TSR = 3.1 and TSR = 3.3, respectively. These deviations are attributed to the increased turbulence intensity and the presence of three-dimensional (3D) vortex structures in experiments that cannot be fully captured in a 2D simulation. Nevertheless, as shown in Fig. 5, the overall trend exhibits strong consistency, and the average percentage error remains within acceptable limits for 2D analyses.

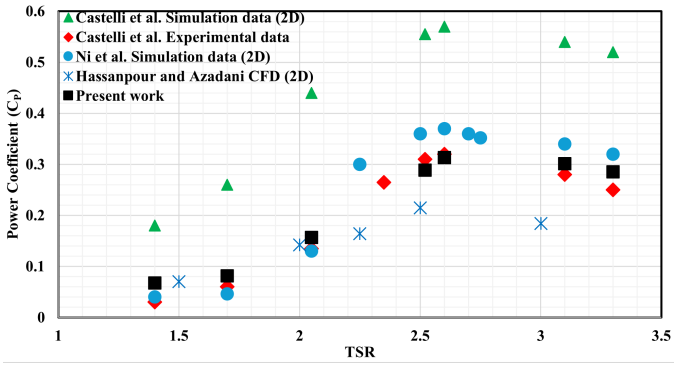

Fig. 5. Comparison of the C_P with both the numerical and experimental study of Castelli *et al.* [50], the numerical studies of Ni *et al.* [62] and Hassanpour and Azadani [63]

3. TAGUCHI METHOD

The Taguchi method is a valuable tool for the robust and efficient optimization of VAWT design and operational parameters. Using orthogonal arrays, the method reduces the number of required experiments, thereby simplifying the optimization process and significantly lowering computational cost and time [64].

Optimizing key parameters such as blade shape and orientation, TSR, and other critical design factors with the Taguchi method enhances turbine performance and efficiency. Additionally, it enables the analysis of parameter interactions, facilitating the development of designs that are robust against signal-to-noise (S/N) factors. In summary, applying the Taguchi method in

VAWT design optimization substantially contributes to improving wind energy generation while maintaining computational efficiency.

In this study, the Taguchi method, as illustrated in the flow chart in Fig. 6, was utilized to optimize the parameters of BSC and β, both of which influence the wind turbine performance. This study investigates the impact of parameters BSC and β, which have notable effects on blade performance as evidenced in the literature. The influence of β in the NACA 0021 blade model, denoted as (+), (−), and neutral, is depicted in Fig. 7. In Fig. 7a, the model is on the tangent line. In Fig. 7b, the leading edge of the blade is directed towards the center of the turbine, defined as the (−) β direction. In Fig. 7c, the trailing edge of the blade, also represents as the (−) β direction, is directed towards the turbine center. Figure 8 illustrates the four different BSC positions employed in this study. In the context of VAWTs, the BSC refers to the location where the blades of the turbine are attached to the central rotor, or "spoke".

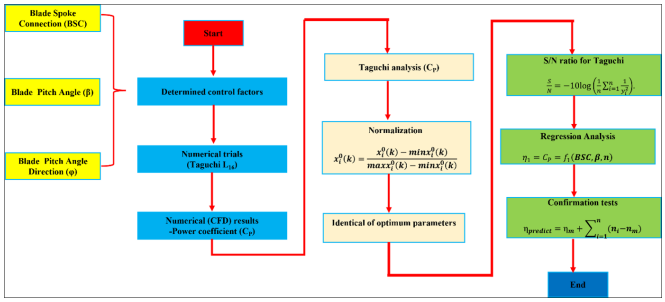

Fig. 6. Flow chart of the Taguchi method

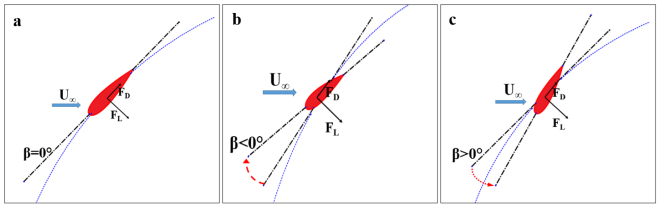

Fig. 7. Schematic illustrating the β for a VAWT blade

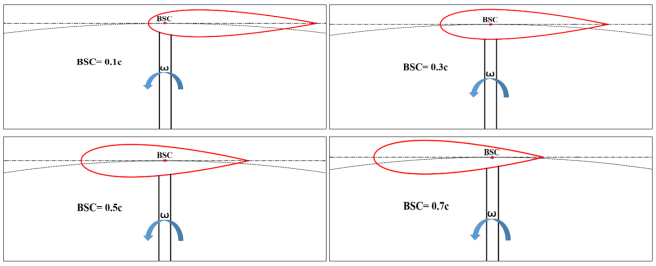

Fig. 8. Schematic representation of various BSC points

The Taguchi method fundamentally comprises three main elements: defining the objective function, identifying design parameters, and utilizing the results of numerical trials (runs) to derive the optimal design parameter, which is subject to S/N ratio analyses. Table 3 details the factors determined using the BSC, β, and φ (turbine blade pitch angle direction) parameters, which constitute the objective function. This study determined the factors of the BSC [35, 36] and β [20, 65, 66] parameters by taking into consideration the works in the literature. In the objective function, the factors BSC, β, and φ are represented as A, B, and C, respectively. One of the key steps in the Taguchi method is generating the orthogonal array [67].

Table 3
Specification of factors and their levels

Control factor		Levels			
		1	2	3	4
A	Blade-spoke connection (BSC)	0.1c	0.3c	0.5c	0.7c
B	Turbine blade pitch angle (β)	2°	4°	6°	8°
C	Turbine blade pitch direction (φ)	(+)	(−)		

By establishing an L_{16} orthogonal array in Table 4, using four levels for the BSC and β factors, and two levels for the φ factor, the study aims to determine both the optimal parameter configuration and the effects of the parameters through 16 numerical trials. Parameters within the S/N objective function, expressed by (5), are defined as indicators of quality measurement. As the BSC and β factors of the VAWT with the highest C_P are identified as the optimal parameters, the "larger-the-better" module is applied for the S/N ratio in (5) [68]

$$\frac{S}{N} = -\log\left(\frac{1}{n}\sum_{i=1}^{n}\frac{1}{y_i^2}\right), \tag{5}$$

where n represents the number of runs and y_i denotes the C_P of the VAWT.

Table 4
Matrix experiment design using the Taguchi method

Run.	Level		
	BSC	β	φ
1	0.1	2	(+)
2	0.1	4	(+)
3	0.1	6	(−)
4	0.1	8	(−)
5	0.3	2	(+)
6	0.3	4	(+)
7	0.3	6	(−)
8	0.3	8	(−)
9	0.5	2	(−)
10	0.5	4	(−)
11	0.5	6	(+)
12	0.5	8	(+)
13	0.7	2	(−)
14	0.7	4	(−)
15	0.7	6	(+)
16	0.7	8	(+)

4. RESULT AND DISCUSSION

4.1. Factor and S/N effects of VAWT

Based on the maximum C_P of the B1 at $\lambda = 2.62$, 16 numerical trials (referred to as "runs") were conducted at this specific TSR, with the corresponding C_P values, S/N ratios, and percentage-based power increments for both B1 and the runs presented in Table 5. The B1 obtained a C_P of 0.313. Given the "larger-the-better" selection for the S/N ratio type, it was observed that models possessing higher S/N ratios also demonstrated elevated C_P values. Specifically, run 3 and run 9 showed significant enhancements in VAWT performance, with improvements of 4.92% and 5.82%, respectively. In contrast, the remaining 11 models generated through the orthogonal array were revealed to negatively influence VAWT performance, illustrating the critical role of these selected parameters in optimizing turbine efficacy.

Table 5
Simulation result for the averaged C_P and S/N ratio

Run	Level			$C_{P,\max}$	S/N ratio	Power increment (%)
	BSC	β	φ			
1	0.1	2	(+)	0.135265	–17.3763	–56.78
2	0.1	4	(+)	0.173263	–15.2259	–44.64
3	0.1	6	(–)	0.328411	–9.6717	4.92
4*	0.1	8	(–)	0.309382	–10.1901	–1.16
5	0.3	2	(+)	0.217345	–13,2570	–30.56
6	0.3	4	(+)	0.169743	–15.4041	–45.77
7*	0.3	6	(–)	0.313661	–10.0708	0.21
8	0.3	8	(–)	0.251019	–12.0059	–19.80
9	0.5	2	(–)	0.331224	–9.5976	5.82
10*	0.5	4	(–)	0.315007	–10.0336	0.64
11	0.5	6	(+)	0.149989	–17.7217	–52.08
12	0.5	8	(+)	0.164154	–16.8240	–47.55
13	0.7	2	(–)	0.316719	–9.9865	1.19
14	0.7	4	(–)	0.262671	–11.6117	–16.08
15*	0.7	6	(+)	0.198315	–14.0529	–36.64
16	0.7	8	(+)	0.132498	–17.5558	–57.67

* Testing

To provide a clearer visualization of how different Blade-BSC positions influence turbine performance, Table 6 summarizes the average, maximum, and minimum C_P values at each BSC level. This presentation allows a direct comparison of BSC effects, independent of other design parameters.

Table 6
The effect of BSC position on average C_P (averaged over all runs at each level)

BSC Level	$C_{P,\text{Avg}}$	$C_{P,\max}$	$C_{P,\min}$
0.1	0.23608	0.3284	0.1352
0.3	0.2374	0.3136	0.1697
0.5	0.2401	0.3312	0.1499
0.7	0.2270	0.3167	0.1324

As derived from Table 7 and illustrated in Fig. 9, the effect levels of each of the three factors are expressed in terms of the mean factor. A high mean value positively impacts the performance of the VAWT. Therefore, the maximum mean levels of each factor help in determining the optimal BSC and β parameters. In this context, as seen in Fig. 9, the highest-level values of the BSC, β, and φ factors have been obtained as 0.5c (A3), 2° (B1), and (–) (C2), respectively.

Table 7
S/N ratio response table (η) for power density based on the larger-is-better criterion

Level	A	B	C
1	0.2366	0.2501	0.1676
2	0.2379	0.2302	0.3035
3	0.2401	0.2476	
4	0.2276	0.2143	
Delta	0.0125	0.0359	0.1359
Rank	3	2	1

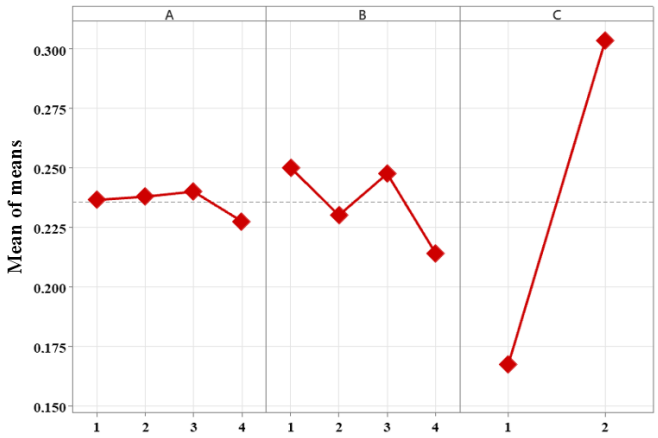

Fig. 9. Mean response plot for control factors

4.2. Analysis of variance

ANOVA in scientific studies about VAWTs evaluates the impact of multiple factors, such as design characteristics, environmental conditions, or installation variables, on the power output or efficiency of the turbines [69]. Until now, the optimal performance of VAWTs has been achieved using the Taguchi method, applying certain factors and levels. In the ANOVA objective function, the set factors allow for determining their respective contribution to the performance of the VAWTs. The percentage contribution ratio (PCR) is calculated as shown in (6). Table 8 presents the contribution amounts of the three factors to VAWTs. The most significant influence on VAWT performance comes from factor φ, contributing 82.07%, while the least influence is

observed from factor β, contributing only 1.17%. The influence of factor BSC is obtained at 3.99%. Additionally, the error was determined to be 12.78%, which is relatively low and considered acceptable within the academic literature [70].

Table 8
Results of ANOVA for power density

Source	DoF	SS	MS	F-test	P	PCR (%)
A	3	0.823	0.274	0.14	0.936	3.99
B	3	4.526	1.509	0.75	0.554	1.17
C	1	109.612	109.612	54.31	0	82.07
Residual error	8	16.146	2.018			12.78
Total	15	131.107				100

$$\%\text{PCR} = \frac{(SS_A - (v_e)(v_A))}{SS_T} \cdot 100. \tag{6}$$

4.3. Correlation and confirmation test

Correlation and regression analysis (RA) aim to enhance the C_P performance through the linear equation established based on the BSC, β, and φ parameters in the objective function. Equation (7) illustrates the relationship between C_P and these factors in the objective function. Equation (8), representing the correlation equation, enables the creation of analytical solutions for all models using the specified factors and levels in the objective function. The C_P values obtained in the confirmation test were divided into two sets: training data and test data. Training for the correlation equation in (8) was conducted without including all models from the orthogonal design, as shown in Table 5, to allow for a confirmation test. Twelve out of sixteen numerical trials were selected as training data to form the correlation equation. The remaining four models were chosen as test data, and confirmation tests were performed using the correlation equation in (8). Additionally, the numerical results and C_P values obtained with RA models are plotted in Figs. 10 and 11, comparing both the training data and test data. The results indicate that the training and test data obtained through RA are quite similar.

$$\eta_1 = C_P = f_1(\text{BSC}, \beta, \varphi). \tag{7}$$

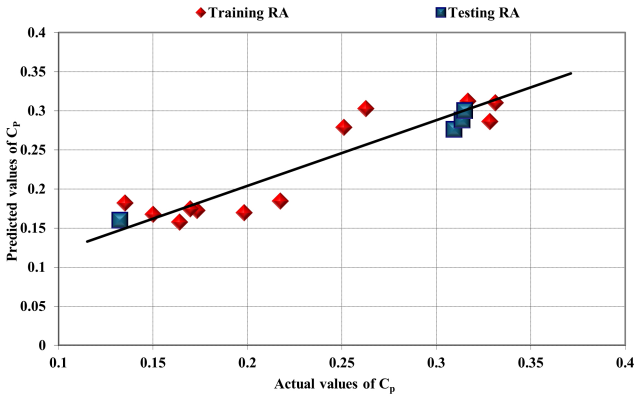

Fig. 10. Predicted and actual C_P profiles of training and testing data

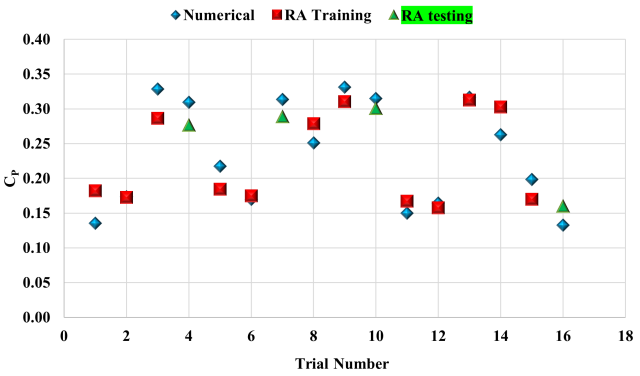

Fig. 11. Comparison of training and testing data obtained from RA with numerical results

The correlation for C_P

$$C_P = 0.0659 + 0.00044 \cdot (A) - 0.01304 \cdot (B) + 0.1298 \cdot (C). \tag{8}$$

RA has been conducted in two stages: training data and test data. To check the accuracy of the statistical analysis solution, it is necessary to determine the error between the training and test data. Equations (9) and (10) define the expressions of coefficient of determination (R^2) and statistical error amount (RMSE), respectively [71]. An R^2 close to 1 and an RMSE close to 0 indicate high reliability of the study. Table 9 presents the statistical analysis of the training and test data derived from RA. Upon examining the results, the R^2 values for the training and test data were found to be 0.922139 and 0.990779, respectively, while the RMSE values were 0.01178 and 0.002482 for the same datasets. These values confirm the reliability of the study.

$$R^2 = 1 - \left(\frac{\sum_{i=1}^{N} (t_i - o_i)^2}{\sum_{i=1}^{N} o_i^2} \right), \tag{9}$$

$$\text{RMSE} = \left(\frac{\sum_{i=1}^{N} (t_i - o_i)^2}{o_i} \right)^{\frac{1}{2}}. \tag{10}$$

Table 9
Statistical results of RA

	RA	
	RMSE	R^2
Training	0.01178	0.922139
Testing	0.002482	0.990779

4.4. Aerodynamic examination

In this section, the run 9 (Optimal) VAWT model with A3B1C2 parameters is compared aerodynamically with the B1 model. Figure 12 illustrates the torques produced by a single blade of run 9 and B1 over one complete revolution at a 2.62λ. For detailed analysis, one complete revolution in Fig. 12 is divided

into four different azimuth angle (θ) ranges: upwind: $45° < \theta < 135°$; leeward: $135° < \theta < 225°$; downwind: $225° < \theta < 315°$; windward: $315° < \theta < 45°$ [72].

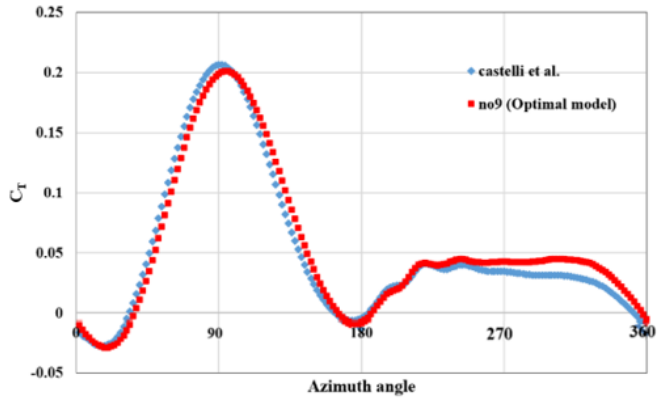

Fig. 12. Profiles of C_T with θ azimuth angle within a rotation cycle for one blade of the optimal (Run 9) and conventional model

Upon examining in Fig. 12, it was observed that the B1 blade produced higher torque than the run 9 up to 90° in the first half of upwind. However, after 90°, it was noticed that run 9 had higher performance at almost all azimuth angles. Notably, the run 9 was seen to generate markedly higher torque than B1 from the leeward section (90° to 180°) and the beginning of the downwind till the end of one complete revolution (360°). This condition explains the 5.82% higher C_P performance of the run 9 shown in Table 5 compared to the B1.

To physically understand and aerodynamically verify that the BSC and β parameters improve VAWT performance, instantaneous turbulence kinetic energy distribution values were calculated. Figure 13 shows the optimal VAWT instantaneous turbulence kinetic energy with straight turbine blades at the same azimuth angle for one complete revolution. In the results, the vortices formed in the trailing edge region of the traditional turbine blade are relatively slightly more intense than the run 9 at 60 and 90° azimuth angles. At a 150° azimuth angle, the vorticity intensity and width of the optimal blade are notably greater

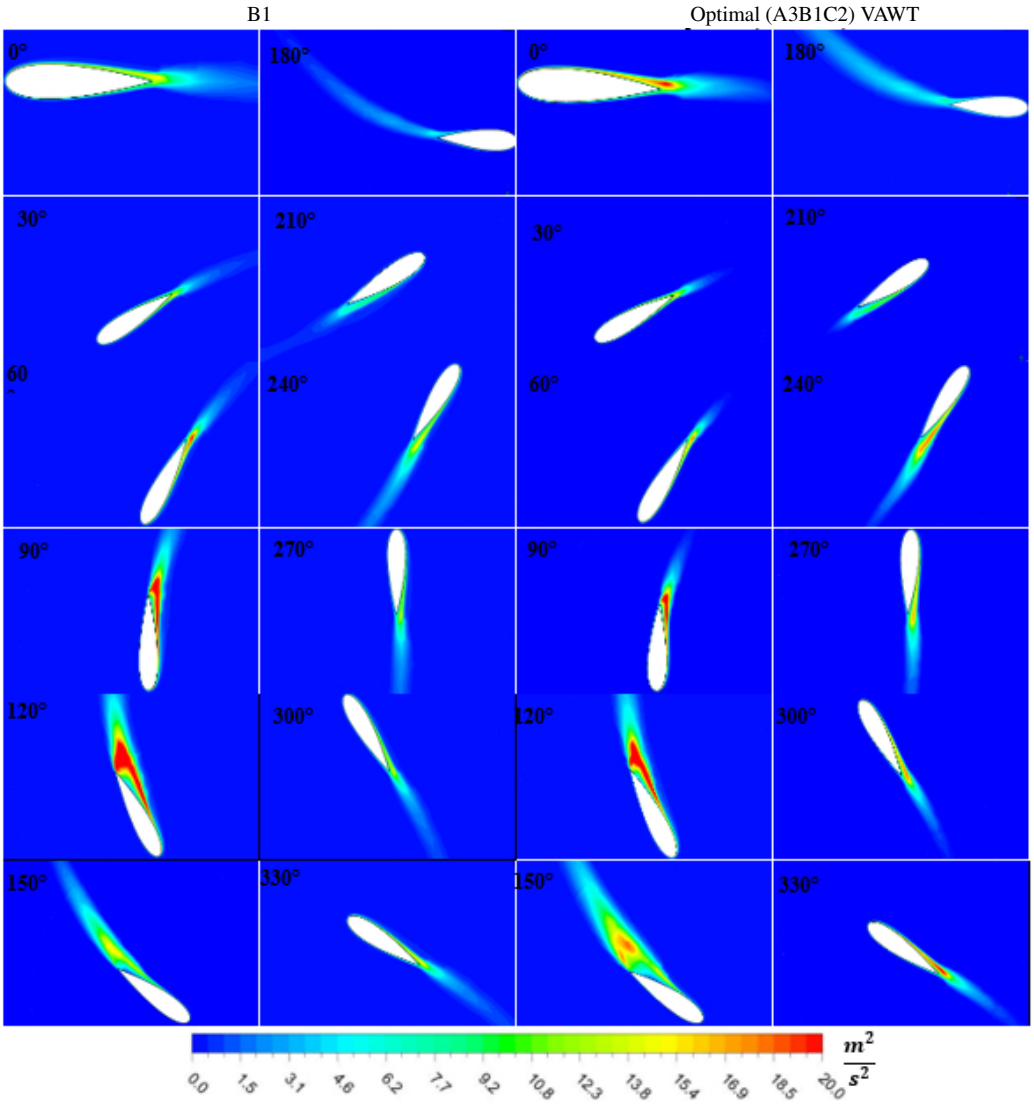

Fig. 13. Turbulence kinetic energy graph of one blade of B1 and the optimal model for one entire revolution

than those of the conventional blade. Between 180 and 210° azimuth angles, both models have exhibited similar behaviors. However, between 240 and 330° azimuth angles, despite the vortex widths of the conventional blade and the optimal blade being similar due to the turbine structure, the vortex intensity of the optimal blade is considerably higher than the conventional blade at these angles. In the majority of azimuth angles, the fact that run 9 generates more intense vortices compared to the traditional model is corroborated by Fig. 13.

5. CONCLUSIONS

This study presents a comprehensive investigation aimed at enhancing the aerodynamic performance of VAWTs by simultaneously optimizing three key parameters, BSC, β, and φ, using the Taguchi method. Unlike previous studies that examined these parameters separately, this research integrates them within a unified statistical optimization framework. The aerodynamic effects of different configurations were evaluated through unsteady Reynolds-averaged Navier-Stokes (URANS) simulations conducted in ANSYS Fluent. Flow behaviors were analyzed in detail, and performance was quantitatively assessed based on C_P.

Key findings of this study can be summarized as follows:

- The Taguchi method proved to be a robust and efficient optimization tool for reducing the number of simulation trials while identifying the most influential factor combinations in VAWT design.
- The optimal parameter combination was achieved in the A3B1C2 configuration, corresponding to BSC = 0.5c, β = 2°, and $\varphi = (-)$. This setup resulted in a 5.82% increase in C_P compared to the B1, demonstrating clear aerodynamic advantages.
- According to ANOVA results, φ had the most dominant impact on turbine performance with a contribution rate of 82.07%, while BSC and β had smaller yet relevant effects at 3.99% and 1.17%, respectively. These findings suggest that β direction is a critical factor in flow interaction optimization.
- RA confirmed the validity and reliability of the optimization results. The model exhibited excellent predictive capability, with R^2 values of 0.9221 (training) and 0.9908 (testing), and low RMSE values, reinforcing the model accuracy in C_P estimation.
- Aerodynamic comparisons between the optimized and baseline configurations showed that the optimized model generated higher torque, especially in the leeward and downwind phases, which contributed significantly to overall C_P improvement.

FUTURE RESEARCH DIRECTIONS

The current 2D analysis has effectively revealed the influence of BSC positions and β variations on the aerodynamic performance of the VAWT blade. Building upon this foundation, future studies will extend the scope to 3D simulations to investigate the flow turbulence and vortex structures in the junction region between the strut and blade.

REFERENCES

[1] S. Sachar, P. Doerffer, P. Flaszyński, K. Doerffer, J. Grzelak, and A. Reiter, "Analysis of a novel vertical axis twin-rotor wind turbine performance in an urban environment," *Bull. Pol. Acad. Sci. Tech. Sci.*, vol. 73, no. 5, p. e155039, Sep. 2025, doi: 10.24425/BPASTS.2025.155039.

[2] H. Seifi Davari, R.M. Botez, M. Seify Davari, H. Chowdhury, and H. Hosseinzadeh, "Blade height impact on self-starting torque for Darrieus vertical axis wind turbines," *Energy Convers. Manag.-X*, vol. 24, p. 100814, Oct. 2024, doi: 10.1016/J.ECMX.2024.100814.

[3] M. Seyhan, H.E. Tanürün, N. Aydin, and E. Ayyildiz, "Strategic site selection for biohydrogen production: Enhancing rural sustainability through agricultural biomass," *Energy Sustain. Dev.*, vol. 89, p. 101838, Dec. 2025, doi: 10.1016/J.ESD.2025.101838.

[4] P. Strojny, "Study on the efficiency of small-scale wind turbine with rotor adapted for low wind speeds," *Bull. Pol. Acad. Sci. Tech. Sci.*, vol. 72, no. 6, p. e151954, 2024, doi: 10.24425/BPASTS.2024.151954.

[5] W.H. Chen, C.Y. Chen, C.Y. Huang, and C.J. Hwang, "Power output analysis and optimization of two straight-bladed vertical-axis wind turbines," *Appl. Energy*, vol. 185, pp. 223–232, Jan. 2017, doi: 10.1016/j.apenergy.2016.10.076.

[6] M. Seyhan and H.E. Tanürün, "Experimental optimization of the SG6043 airfoil for horizontal axis wind turbine using Schmitz equations," *Int. J. Energy Stud.*, vol. 9, no. 4, pp. 619–636, Dec. 2024, doi: 10.58559/IJES.1552364.

[7] V. Demırcı, F.E. Kan, M. Seyhan, and M. Sarıoğlu, "The effects of the location of the leading-edge tubercles on the performance of horizontal axis wind turbine," *Energy Convers. Manag.*, vol. 324, p. 119178, Jan. 2025, doi: 10.1016/J.ENCONMAN.2024.119178.

[8] H. Seifi Davari, R.M. Botez, M. Seify Davari, H. Chowdhury, and H. Hosseinzadeh, "Numerical and experimental investigation of Darrieus vertical axis wind turbines to enhance self-starting at low wind speeds," *Results Eng.*, vol. 24, p. 103240, Dec. 2024, doi: 10.1016/J.RINENG.2024.103240.

[9] L. Kuang *et al.*, "Systematic investigation of effect of rotor solidity on vertical-axis wind turbines: Power performance and aerodynamics analysis," *J. Wind Eng. Ind. Aerodyn.*, vol. 233, p. 105284, Feb. 2023, doi: 10.1016/J.JWEIA.2022.105284.

[10] T. Krysiński, Z. Buliński, and A.J. Nowak, "Numerical modeling and preliminary validation of drag-based vertical axis wind turbine," *Arch. Thermodyn.*, vol. 36, no. 1, pp. 19–38, Oct. 2015, doi: 10.1515/AOTER-2015-0002.

[11] H.E. Tanürün, "Improvement of vertical axis wind turbine performance by using the optimized adaptive flap by the Taguchi method," Energy Sources, Part A: Recovery, *Util. Environ. Eff.*, vol. 46, no. 1, pp. 71–90, Dec. 2024, doi: 10.1080/15567036.2023.2279264.

[12] M. Bashir Ali Bashir, I. Ali, and A. Hussain Rajpar, "Performance analysis of micro-vertical axis wind turbine integrated with upstream omnidirectional wind deflector," *Arab. J. Sci. Eng.*, vol. 47, no. 12, pp. 16239–16249, Dec. 2022, doi: 10.1007/S13369-022-06896-1.

[13] B. Hand, G. Kelly, and A. Cashman, "Aerodynamic design and performance parameters of a lift-type vertical axis wind turbine: A comprehensive review," *Renew. Sustain. Energy Rev.*, vol. 139, p. 110699, Apr. 2021, doi: 10.1016/J.RSER.2020.110699.

[14] H. Seifi Davari, M. Seify Davari, R.M. Botez, and H. Chowdhury, "Advancements in vertical axis wind turbine technologies: A comprehensive review," *Arab. J. Sci. Eng.*, vol. 50, no. 4, pp. 2169–2216, Feb. 2025, doi: 10.1007/S13369-024-09723-X.

[15] Z. Xu *et al.*, "Experimental and numerical investigation on aerodynamic performance of a novel disc-shaped wind rotor for the small-scale wind turbine," *Energy Convers. Manag.*, vol. 175, pp. 173–191, Nov. 2018, doi: 10.1016/J.ENCONMAN.2018.09.003.

[16] A. Zhankeldi, B. Kozhageldiyev, E. Askarov, R. Mukanov, and B. Bazarbay, "Innovative fixed-axle Savonius wind turbine for enhanced efficiency and durability," *Polityka Energ.*, vol. 28, no. 3, pp. 51–78, 2025, doi: 10.33223/epj/205943.

[17] A. Posa, "Secondary flows in the wake of a vertical axis wind turbine of solidity 0.5 working at a tip speed ratio of 2.2," *J. Wind Eng. Ind. Aerodyn.*, vol. 213, p. 104621, Jun. 2021, doi: 10.1016/J.JWEIA.2021.104621.

[18] Rezaeiha, H. Montazeri, and B. Blocken, "Towards optimal aerodynamic design of vertical axis wind turbines: Impact of solidity and number of blades," *Energy*, vol. 165, pp. 1129–1148, Dec. 2018, doi: 10.1016/J.ENERGY.2018.09.192.

[19] Y. Yang, Z. Guo, Q. Song, Y. Zhang, and Q. Li, "Effect of Blade Pitch Angle on the Aerodynamic Characteristics of a Straight-bladed Vertical Axis Wind Turbine Based on Experiments and Simulations," *Energies*, vol. 11, no. 6, p. 1514, Jun. 2018, doi: 10.3390/EN11061514.

[20] Q. Li *et al.*, "Study on power performance for straight-bladed vertical axis wind turbine by field and wind tunnel test," *Renew. Energy*, vol. 90, pp. 291–300, May 2016, doi: 10.1016/J.RENENE.2016.01.002.

[21] A. Carbó Molina, T. De Troyer, T. Massai, A. Vergaerde, M.C. Runacres, and G. Bartoli, "Effect of turbulence on the performance of VAWTs: An experimental study in two different wind tunnels," *J. Wind Eng. Ind. Aerodyn.*, vol. 193, p. 103969, Oct. 2019, doi: 10.1016/J.JWEIA.2019.103969.

[22] Song, G. Wu, W. Zhu, and X. Zhang, "Study on Aerodynamic Characteristics of Darrieus Vertical Axis Wind Turbines with Different Airfoil Maximum Thicknesses Through Computational Fluid Dynamics," *Arab. J. Sci. Eng.*, vol. 45, no. 2, pp. 689–698, Feb. 2020, doi: 10.1007/S13369-019-04127-8.

[23] H. Seifi Davari, S. Kouravand, M. Seify Davari, and Z. Kamalnejad, "Numerical investigation and aerodynamic simulation of Darrieus H-rotor wind turbine at low Reynolds numbers," *Energy Sources, Part A-Recovery, Util. Environ. Eff.*, vol. 45, no. 3, pp. 6813–6833, Aug. 2023, doi: 10.1080/15567036.2023.2213670.

[24] F. Kaya, H. E. Tanürün, and A. Acır, "Numerical Investigation of Radius Dependent Solidity Effect on H-Type Vertical Axis Wind Turbines," *Politeknik Dergi.*, vol. 25, no. 3, pp. 1007–1019, Oct. 2022, doi: 10.2339/POLITEKNIK.799767.

[25] H. E. Tanürün, "Taguchi Yöntemiyle Sağlamlık Oranının Dikey Eksenli Rüzgâr Türbini Performansına Olan Etkisinin Sayısal Olarak İncelenmesi," *J. Mater. Mechatron. A,* vol. 4, no. 2, pp. 355–372, Dec. 2023, doi: 10.55546/JMM.1295748.

[26] D. Moher, A. Liberati, J. Tetzlaff, and D. G. Altman, "Preferred reporting items for systematic reviews and meta-analyses: The PRISMA statement," *Ann. Intern. Med.*, vol. 151, no. 4, pp. 264–269, Jan. 2009, doi: 10.7326/0003-4819-151-4-200908180-00135.

[27] J. Zhou, L. Wu, C. Zhang, J. Wang, Y. Liu, and L. Ping, "Ultrasound guided axillary vein catheterization versus subclavian vein cannulation with landmark technique: A PRISMA-compliant systematic review and meta-analysis," *Medicine*, vol. 101, no. 43, p. E31509, Oct. 2022, doi: 10.1097/MD.0000000000031509.

[28] S. Taneja, P. Jaggi, S. Jewandah, and E. Ozen, "Role of Social Inclusion in Sustainable Urban Developments: An Analyse by PRISMA Technique," *Int. J. Des. Nature Ecodyn.*, vol. 17, no. 6, pp. 937–942, Dec. 2022, doi: 10.18280/IJDNE.170615.

[29] N. Franchina, O. Kouaissah, G. Persico, and M. Savini, "Three-Dimensional CFD Simulation and Experimental Assessment of the Performance of a H-Shape Vertical-Axis Wind Turbine at Design and Off-Design Conditions," *Int. J. Turbomach. Propuls. Power*, vol. 4, no. 3, p. 30, Sep. 2019, doi: 10.3390/IJTPP4030030.

[30] D. Keisar, I. Arava, and D. Greenblatt, "Dynamic-stall-driven vertical axis wind turbine: An experimental parametric study," *Appl. Energy*, vol. 365, p. 123199, Jul. 2024, doi: 10.1016/J.APENERGY.2024.123199.

[31] Y. Hara, N. Horita, S. Yoshida, H. Akimoto, and T. Sumi, "Numerical Analysis of Effects of Arms with Different Cross-Sections on Straight-Bladed Vertical Axis Wind Turbine," *Energies*, vol. 12, no. 11, pp. 1–24, 2019, doi: 10.3390/en12112106.

[32] Y. Jiang, C. He, P. Zhao, and T. Sun, "Investigation of Blade Tip Shape for Improving VAWT Performance," *J. Mar. Sci. Eng.*, vol. 8, no. 3, p. 225, 2020, doi: 10.3390/jmse8030225.

[33] Aihara, V. Mendoza, A. Goude, and H. Bernhoff, "A numerical study of strut and tower influence on the performance of vertical axis wind turbines using computational fluid dynamics simulation," *Wind Energy*, vol. 25, no. 5, pp. 897–913, May 2022, doi: 10.1002/we.2704.

[34] L. Santamaría, J.M. Fernández Oro, K.M. Argüelles Díaz, A. Meana-Fernández, B. Pereiras, and S. Velarde-Suárez, "Novel methodology for performance characterization of vertical axis wind turbines (VAWT) prototypes through active driving mode," *Energy Convers. Manag.*, vol. 258, p. 115530, Apr. 2022, doi: 10.1016/j.enconman.2022.115530.

[35] Aihara, V. Mendoza, A. Goude, and H. Bernhoff, "Comparison of Three-Dimensional Numerical Methods for Modeling of Strut Effect on the Performance of a Vertical Axis Wind Turbine," *Energies*, vol. 15, no. 7, p. 2361, Mar. 2022, doi: 10.3390/en15072361.

[36] W. Miao *et al.*, "Recommendation for strut designs of vertical axis wind turbines: Effects of strut profiles and connecting configurations on the aerodynamic performance," *Energy Convers. Manag.*, vol. 276, p. 116436, Jan. 2023, doi: 10.1016/j.enconman.2022.116436.

[37] A.F.P. Ribeiro, C.S. Ferreira, and D. Casalino, "Vertical axis wind turbine wake steering by pitched struts and blades," *J. Phys.: Conf. Ser.*, vol. 2767, no. 9, p. 092004, Jun. 2024, doi: 10.1088/1742-6596/2767/9/092004.

[38] L. Santamaría, L. Suarez Fernandez, M. Garcia-Diaz, J. González Pérez, and M. Galdo, "Bioinspired Trailing Edge Serrations for Vertical Axis Wind Turbine Blades in Urban Environments: Performance Effects," *J. Bionic Eng.*, vol. 22, no. 2, pp. 822–837, Feb. 2025, doi: 10.1007/s42235-025-00660-5.

[39] A. Bianchini, G. Ferrara, and L. Ferrari, "Pitch optimization in small-size Darrieus wind turbines," *Energy Procedia*, vol. 81, pp. 122–132, 2015, doi: 10.1016/j.egypro.2015.12.067.

[40] Y.-L. Xu, Y.-X. Peng, and S. Zhan, "Optimal blade pitch function and control device for high-solidity straight-bladed vertical axis

wind turbines," *Appl. Energy*, vol. 242, pp. 1613–1625, Mar. 2019, doi: 10.1016/j.apenergy.2019.03.151.

[41] M.M. Elsakka, D.B. Ingham, L. Ma, and M. Pourkashanian, "CFD analysis of the angle of attack for a vertical axis wind turbine blade," *Energy Convers. Manag.*, vol. 182, pp. 154–165, Feb. 2019, doi: 10.1016/j.enconman.2018.12.054.

[42] F. Ardaneh, A. Abdolahifar, and S.M.H. Karimian, "Numerical analysis of the pitch angle effect on the performance improvement and flow characteristics of the 3-PB Darrieus vertical axis wind turbine," *Energy*, vol. 239, p. 122339, Jan. 2022, doi: 10.1016/j.energy.2021.122339.

[43] Hunt *et al.*, "An experimental evaluation of the interplay between geometry and scale on cross-flow turbine performance," *Renew. Sustain. Energy Rev.*, vol. 206, p. 114848, Dec. 2024, doi: 10.1016/j.rser.2024.114848.

[44] K. Ma, J. Wang, and K. Lin, "A novel variable pitch control strategy to improve the aerodynamics of vertical axis wind turbine," *Phys. Fluids*, vol. 37, no. 3, p. 035125, Mar. 2025, doi: 10.1063/5.0254998.

[45] H.Y. Peng, Z.D. Han, H.J. Liu, K. Lin, and H.F. Lam, "Assessment and optimization of the power performance of twin vertical axis wind turbines via numerical simulations," *Renew. Energy*, vol. 147, pp. 43–54, Mar. 2020, doi: 10.1016/j.renene.2019.08.124.

[46] H.Y. Peng, M.N. Liu, H.J. Liu, and K. Lin, "Optimization of twin vertical axis wind turbines through large eddy simulations and Taguchi method," *Energy*, vol. 240, p. 122560, Feb. 2022, doi: 10.1016/j.energy.2021.122560.

[47] J. Zhang, C. Wang, W. Liu, J. Zhu, Y. Yan, and H. Zhao, "Optimization of the Energy Capture Performance of the Lift-Drag Hybrid Vertical-Axis Wind Turbine Based on the Taguchi Experimental Method and CFD Simulation," *Sustainability*, vol. 15, no. 11, p. 8848, May 2023, doi: 10.3390/su15118848.

[48] S. Rasekh, S.K. Aliabadi, and M.O.L. Hansen, "Toward improving the performance of a variable pitch vertical axis wind turbine (VP-VAWT), Part 1: Sensitivity analysis using Taguchi-CFD approach," *Ocean Eng.*, vol. 279, p. 114478, Jul. 2023, doi: 10.1016/j.oceaneng.2023.114478.

[49] X. Lu and S. Xu, "Performance optimization of vertical axis wind turbine based on Taguchi method, improved differential evolution algorithm and Kriging model," *Energy Sources Pt A: Recovery, Util. Environ. Eff.*, vol. 46, no. 1, pp. 2792–2810, 2024, doi: 10.1080/15567036.2024.2308655.

[50] M. Raciti Castelli, A. Englaro, and E. Benini, "The Darrieus wind turbine: Proposal for a new performance prediction model based on CFD," *Energy*, vol. 36, no. 8, pp. 4919–4934, 2011, doi: 10.1016/j.energy.2011.05.036.

[51] N. Kashani, M. Mirhosseini, R. Ahmadi, and H. Mirzaeian, "Performance Improvement of Hybrid Vertical Axis Wind Turbines Equipped With J-Shaped Blades," *Energy Sci. Eng.*, vol. 13, no. 9, pp. 4433–4444, Sep. 2025, doi: 10.1002/ese3.70185.

[52] M. Baghdadi, S. Elkoush, B. Akle, and M. Elkhoury, "Dynamic shape optimization of a vertical-axis wind turbine via blade morphing technique," *Renew. Energy*, vol. 154, pp. 239–251, Jul. 2020, doi: 10.1016/j.renene.2020.03.015.

[53] W. Hao, M. Bashir, C. Li, and C. Sun, "Flow control for high-solidity vertical axis wind turbine based on adaptive flap," *Energy Convers. Manag.*, vol. 249, p. 114845, Dec. 2021, doi: 10.1016/j.enconman.2021.114845.

[54] E.T. Chullai, S. Maity, and B.K. Sarkar, "Numerical Investigation on a Series of Parabolic Profiles to Arrive at an Optimum Design Based on the Savonius Wind Rotor," *Arab. J. Sci. Eng.*, pp. 1–17, Nov. 2024, doi: 10.1007/s13369-024-09747-3.

[55] W.H. Chen *et al.*, "Optimization of a vertical axis wind turbine with a deflector under unsteady wind conditions via Taguchi and neural network applications," *Energy Convers. Manag.*, vol. 254, p. 115209, Feb. 2022, doi: 10.1016/j.enconman.2022.115209.

[56] N. Davandeh and M.J. Maghrebi, "Leading Edge Radius Effects on VAWT Performance," *J. Appl. Fluid Mech.*, vol. 16, no. 9, pp. 1877–1886, Jul. 2023, doi: 10.47176/jafm.16.09.1626.

[57] K.U. Reddy, B. Deb, and B. Roy, "Experimental Study on Influence of Aspect Ratio and Auxiliary Blade Profile on the Performance of H-Type Darrieus Wind Rotor," *Arab. J. Sci. Eng.*, vol. 49, no. 2, pp. 1913–1929, Feb. 2024, doi: 10.1007/s13369-023-08049-4.

[58] W. Kuczyński, I. Michalska-Pozoga, M. Szczepanek, and K. Chmiel, "Overview of application options for vertical axis wind turbines," *Arch. Thermodyn.*, vol. 44, no. 4, pp. 665–704, 2023, doi: 10.24425/ather.2023.149737.

[59] K. Rogowski, R. Maroński, and J. Piechna, "Numerical Analysis of a Small-Size Vertical-Axis Wind Turbine Performance and Averaged Flow Parameters Around the Rotor," *Arch. Mech. Eng.*, vol. 64, no. 2, pp. 205–218, Jun. 2017, doi: 10.1515/meceng-2017-0013.

[60] K. Rogowski, M.O.L. Hansen, and P. Lichota, "2-D CFD Computations of the Two-Bladed Darrieus-Type Wind Turbine," *J. Appl. Fluid Mech.*, vol. 11, no. 4, pp. 835–845, Jul. 2018, doi: 10.29252/jafm.11.04.28383.

[61] E. Marchewka, K. Sobczak, P. Reorowicz, D.S.L. Obidowski, and K. Józwik, "Application of overset mesh approach in the investigation of the Savonius wind turbines with rigid and deformable blades," *Arch. Thermodyn.*, vol. 42, no. 4, pp. 201–216, 2021, doi: 10.24425/ather.2021.139659.

[62] L. Ni, W. Miao, C. Li, and Q. Liu, "Impacts of Gurney flap and solidity on the aerodynamic performance of vertical axis wind turbines in array configurations," *Energy*, vol. 215, p. 118915, 2021, doi: 10.1016/j.energy.2020.118915.

[63] M. Hassanpour and L.N. Azadani, "Aerodynamic optimization of the configuration of a pair of vertical axis wind turbines," *Energy Convers. Manag.*, vol. 238, p. 114069, Jun. 2021, doi: 10.1016/j.enconman.2021.114069.

[64] H. Bayram and H. Yağmur, "The Hydrothermal Performance Investigation of Gasketed Plate Heat Exchangers Using Taguchi, ANOVA, and GRA Methods," *Arab. J. Sci. Eng.*, pp. 1–18, Aug. 2024, doi: 10.1007/s13369-024-09430-7.

[65] Rezaeiha, I. Kalkman, and B. Blocken, "Effect of pitch angle on power performance and aerodynamics of a vertical axis wind turbine," *Appl. Energy*, vol. 197, pp. 132–150, 2017, doi: 10.1016/j.apenergy.2017.03.128.

[66] M.T. Nguyen, F. Balduzzi, and A. Goude, "Effect of pitch angle on power and hydrodynamics of a vertical axis turbine," *Ocean Eng.*, vol. 238, p. 109335, Oct. 2021, doi: 10.1016/j.oceaneng.2021.109335.

[67] H. Tian, X. Dang, D. Meng, B. Tian, and J. Li, "Influence of drilling parameters on bone drilling force and temperature by FE simulation and parameters optimization based Taguchi method," *Alex. Eng. J.*, vol. 75, pp. 115–126, Jul. 2023, doi: 10.1016/j.aej.2023.05.048.

[68] P. Raja, R. Malayalamurthi, and M. Sakthivel, "Experimental investigation of cryogenically treated HSS tool in turning on AISI1045 using fuzzy logic-Taguchi approach," *Bull. Pol. Acad. Sci. Tech. Sci.*, vol. 67, no. 4, pp. 687–696, 2019, doi: 10.24425/bpasts.2019.130178.

[69] R. Çakıroğlu, H.E. Tanürün, A. Acır, F. Üçgül, and S. Olkun, "Optimization of NACA 4412 augmented with a gurney flap by using grey relational analysis," *J. Braz. Soc. Mech. Sci. Eng.*, vol. 45, no. 3, pp. 1–18, Mar. 2023, doi: 10.1007/s40430-023-04089-x.

[70] P. Choudhury, R.N. Ray, T.K. Bandyopadhyay, and B. Bhunia, "Rapid Protocol for Screening of Biocatalyst for Application in Microbial Fuel Cell: A Study with *Shewanella algae*," *Arab. J. Sci. Eng.*, vol. 45, no. 6, pp. 4451–4461, Jun. 2020, doi: 10.1007/s13369-020-04444-3.

[71] R.K. Samal, "Performance of Metaheuristic Algorithms for Wind Resource Modelling: A Comparison Using 80 m Mast Measurements," *Arab. J. Sci. Eng.*, vol. 49, no. 12, pp. 16065–16081, Dec. 2024, doi: 10.1007/s13369-024-08839-4.

[72] H.E. Tanürün and A. Acır, "Investigation of the hydrogen production potential of the H-Darrieus turbines combined with various wind-lens," *Int. J. Hydrogen Energy*, vol. 47, no. 55, pp. 23118–23138, 2022, doi: 10.1016/j.ijhydene.2022.04.196.